Acoustic Liner Drag: A Parametric Study of Conventional Configurations

Brian M. Howerton[1] and Michael G. Jones.[2]
NASA Langley Research Center, Hampton, VA, 23681

Interest in the characterization of the aerodynamic drag performance of acoustic liners has increased in the past several years. This paper details experiments in NASA Langley's Grazing Flow Impedance Tube to quantify the relative drag of several conventional perforate-over-honeycomb liner configurations. For a fixed porosity, facesheet hole diameter and cavity depth are varied to study the effect of each. These configurations are selected to span the range of conventional liner geometries used in commercial aircraft engines. Detailed static pressure and acoustic measurements are made for grazing flows up to M=0.5 at 140 dB SPL for tones between 400 and 2800 Hz. These measurements are used to calculate a resistance factor (λ) for each configuration. Analysis shows a correlation between perforate hole size and the resistance factor but cavity depth seems to have little influence. Acoustic effects on liner drag are observed to be limited to the lower Mach numbers included in this investigation.

Nomenclature

a	=	duct width
b	=	duct height
d_h	=	duct hydraulic diameter
D_{liner}	=	total liner drag
$D_{pressure}$	=	pressure drag
$D_{skin\ friction}$	=	skin friction drag
γ	=	ratio of specific heats
λ	=	resistance factor
l	=	length of core chambers (cavity depth)
k	=	free space wavenumber
M	=	centerline flow Mach number
p_{static}	=	static pressure, absolute
p	=	static pressure, differential
q	=	dynamic pressure
x	=	streamwise duct coordinate

I. Introduction

In the past, the aerodynamic drag imparted by placing acoustic liners in an aircraft engine was tolerated as a necessary penalty in order to meet the required certification noise levels. It is generally accepted that such liners inevitably increase drag relative to when those same areas are covered with a smooth surface.[1] Research by Drouin has also shown that liner drag can also be influenced by the ambient acoustic field.[2] If this acoustic effect results in significant additional drag, new constraints may be required on liner designs to mitigate the associated fuel burn penalty. New aircraft propulsion concepts (open-rotor, distributed electric) may lead to airframe designs where external liners are required to meet community noise goals.[3] Thus, a better understanding of the magnitude of the drag penalty associated with acoustic liners is required to rank their importance in developing drag reduction techniques for future aircraft. The purpose of the current study is (1) to validate a test method for evaluation of liner drag, and (2) to conduct tests to investigate the drag penalty for conventional, perforate-over-honeycomb liners. The

[1] Research Scientist, Structural Acoustics Branch, MS 463, Senior Member AIAA.
[2] Senior Research Scientist, Structural Acoustics Branch, MS 463, Associate Fellow AIAA.

eventual goal is to fabricate and test more radical concepts that vary the perforation geometry and may offer some drag reduction benefits. Advances in three-dimensional (3-D) printing allow for parametric studies of these concepts to develop an empirical database of geometric variations ahead of the formulation of analytical models of liner drag. Due diligence, however, must be given to verify the acoustic performance of these printed liners ensuring that the relevant physics are captured. Thus, an additional goal of this study is to compare predicted and educed impedance spectra for these conventional liners employing printed facesheets to verify construction methods in addition to the aerodynamic measurements.

II. Liner Drag Measurements

Liner drag can be separated into two components as shown in Eq. 1,

$$D_{liner} = D_{skin\ friction} + D_{pressure} \quad (1)$$

where the skin friction component is primarily due to the shear stress between the flow and the liner surface (facesheet) which acts like a distributed roughness. The pressure component is dominated by the hydrodynamic effect of flow into and out of the liner cavities and facesheet orifices. Various methods have been employed in the past to measure these quantities in grazing flow. Direct measurements of total drag can be performed using a force balance approach as in Wilkinson.[4] Indirect methods also exist that look at changes to the surface boundary layer profile such as the momentum thickness and Clauser-type, law-of-the-wall analysis of Roberts.[5]

For this investigation, the relative drag of each configuration will be determined by measuring differences in the static pressure drop along the duct wall opposite of the liner sample. This method can be applied to small ducts with fully-developed, turbulent flow and is similar to Nikuradse's approach when studying roughness in pipes.[6] With the static pressure data and some flow parameters, one can compute the duct's resistance factor, λ (also known as the 'friction factor'), given by the following:

$$\lambda = \frac{dp}{dx}\frac{d_h}{q} \quad (2)$$

using the hydraulic diameter of the flow duct for d_h:

$$d_h = \frac{2ab}{a+b} \quad (3)$$

and the compressible form for q:

$$q = \frac{\gamma}{2} p_{static} M^2 \quad (4)$$

The non-dimensional nature of λ allows the static pressure data to be normalized; taking out the run-to-run effects of slightly varying duct Mach number and static pressure.

III. Experiment

The experimental investigation involves testing of three liner facesheet configurations in conjunction with two liner cores in the NASA Langley Grazing Flow Impedance Tube (GFIT). For each facesheet/core combination, a static pressure survey is performed along the length of the GFIT along with a higher accuracy measurement of the static pressure drop across the liner. A hardwall sample (HW) is included to provide a reference baseline.

A. Facesheet Construction

Each sheet has a constant 8 percent open area (POA) and a sheet thickness of 1.0 mm. Three perforate sizes of nominally 1.0 mm, 0.7 mm and 0.5 mm diameter are evaluated. They are labeled S1, S2 and S3, respectively. The active area for each facesheet is nominally 50.8 mm x 435.2 mm with overall dimensions of 64.0 mm. x 460.8 mm. Figure 1 shows S1 placed on top of one of the core cavities. Figure 2 is a close-up of the three facesheets showing relative differences in hole size and spacing. The facesheets were 3-D printed from photopolymer resin using a stereolithography (SLA) process with the flow surface sanded to ensure a smooth finish.

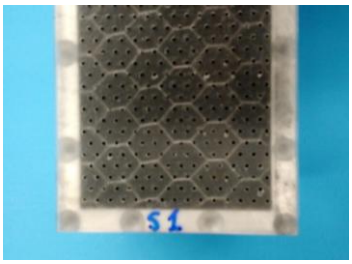

Figure 1. Sample facesheet S1 overlaid on a core cavity.

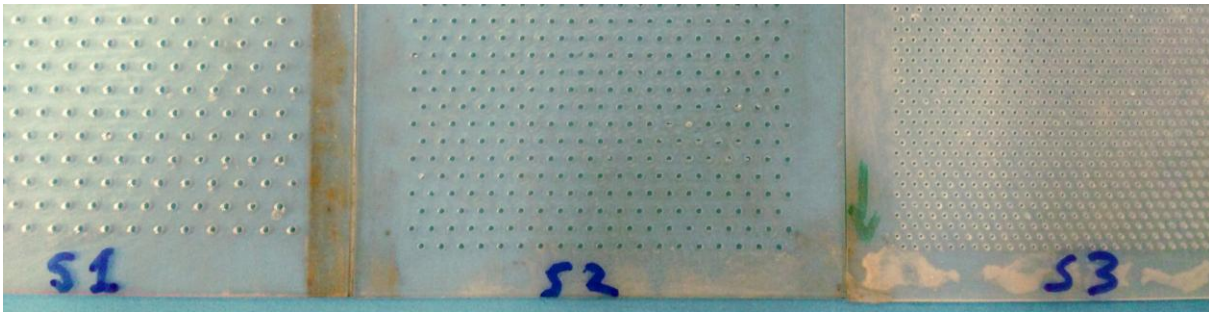

Figure 2. Liner sample facesheets S1 (left), S2 (center) and S3 (right) detail.

B. Liner Core Construction

These facesheets were used over two metallic liner cores of similar construction (same outer dimensions and honeycomb cell size) but with different honeycomb cavity depths. The liner cores were components from a previous investigation that were repurposed for this experiment. Core C1 has a cavity depth of 38.1 mm while C2 uses a 76.2 mm deep honeycomb. Figure 3 shows photos of the two liner cores to highlight the internal construction and relative depths. To allow for rapid changes of liner configuration, the facesheets are not bonded to the core structure but clamped by their long edges as part of installation in the test rig.

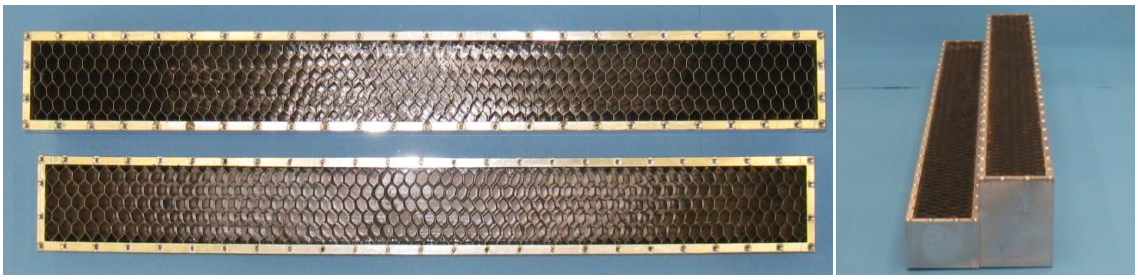

Figure 3. Liner sample core cavities C1 (lower) and C2 (upper) with internal honeycomb.

Note that the cores were constructed for the full length of the GFIT test window (614.4 mm) while the facesheets are only 460.8 mm long. A filler blank was fabricated from the same resin as the facesheets to cover the remaining portion of the core. A summary of the key parameters for each liner configuration is given in Table 1.

Configuration	S1C1	S1C2	S2C1	S2C2	S3C1	S3C2
Hole diameter (mm)	1.0	1.0	0.7	0.7	0.5	0.5
Cavity depth (mm)	38.1	76.2	38.1	76.2	38.1	76.2

Table 1. Liner sample parameters.

C. Grazing Flow Impedance Tube (GFIT)

The Grazing Flow Impedance Tube (GFIT) is a unique facility originally constructed to determine the acoustic characteristics of noise reduction treatments for aircraft jet engine nacelles and nozzles. The facility is a small wind tunnel with a 50.8 mm by 63.5 mm rectangular cross section. The flow path (see Figure 4) is a straight duct with a 12-driver upstream acoustic source section, interchangeable lengths of blank duct, a test section holding the liner sample and an array of 95 measurement microphones leading to a 6-driver downstream source section and anechoic terminating diffuser. Pressurized, heated air is supplied to the entrance of the GFIT while a vacuum system is used at the duct exit to 'pull' the flow out of the tube. This arrangement allows for the static pressure at the test section to be near ambient at all flow velocities while also creating an adiabatic wall condition. In its current configuration, samples can be tested at grazing flow velocities from 0 to Mach 0.6 and sound pressure levels up to 150 dB for the frequency range between 400 and 3000 Hz.

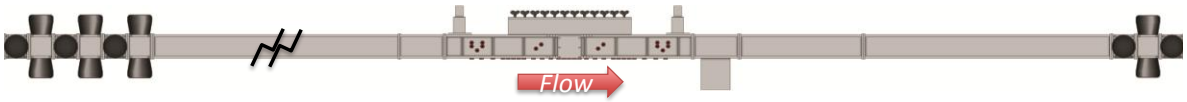

Figure 4. Sketch of the NASA Langley Grazing Flow Impedance Tube (GFIT).

This investigation also makes use of the array of 80 static pressure ports located along the lower wall of the duct to measure the axial pressure distribution. Pressures from these ports are simultaneously sampled by a series of transducers with a +/- 17 kPa range and 0.05% FS accuracy with a fixed sample rate of 100 Hz. Figure 5 shows a representative plot of the complete GFIT static pressure distribution for the baseline smooth hardwall case. The transition from positive to negative pressure nominally occurs at the center of the test section (x = 4.343 m).

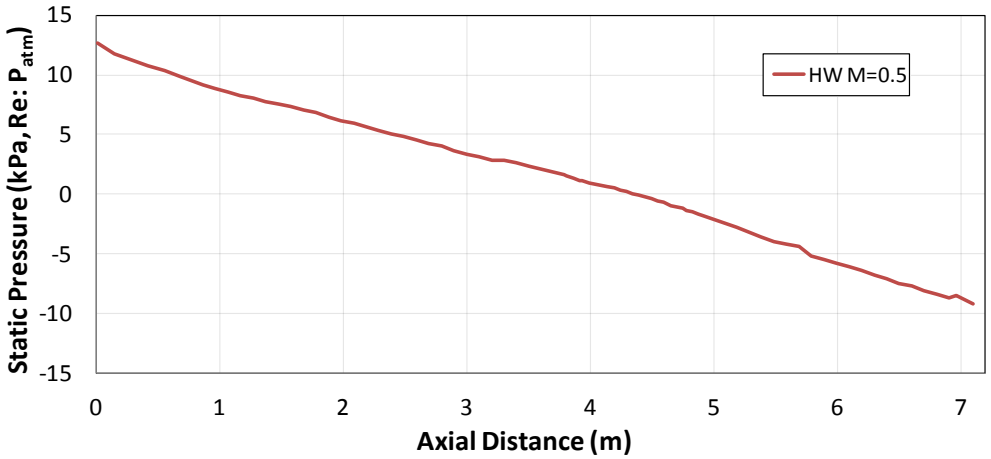

Figure 5. GFIT Static Pressure Distribution, Hardwall sample, M=0.5, No Acoustic Excitation.

A plot of the axial pressure distribution in the test section for the hardwall case is shown in Figure 6. Two ports, one located near the entrance and the other located near the exit of the test section (separated axially by 1.07 m) are also connected to a high-accuracy, differential pressure gauge to measure the static pressure drop between these two locations. This gauge samples at a much slower rate (~10 Hz) but with its smaller 0-6900 Pa range and 0.01% FS accuracy, measurement uncertainty is reduced by a factor of 12.5. A sketch of the test section is included above the plot showing the relative location of the liner and the ports used to compute the static pressure drop (ΔP). The high-resolution measurement points are designated as Port 37 and Port 59, respectively.

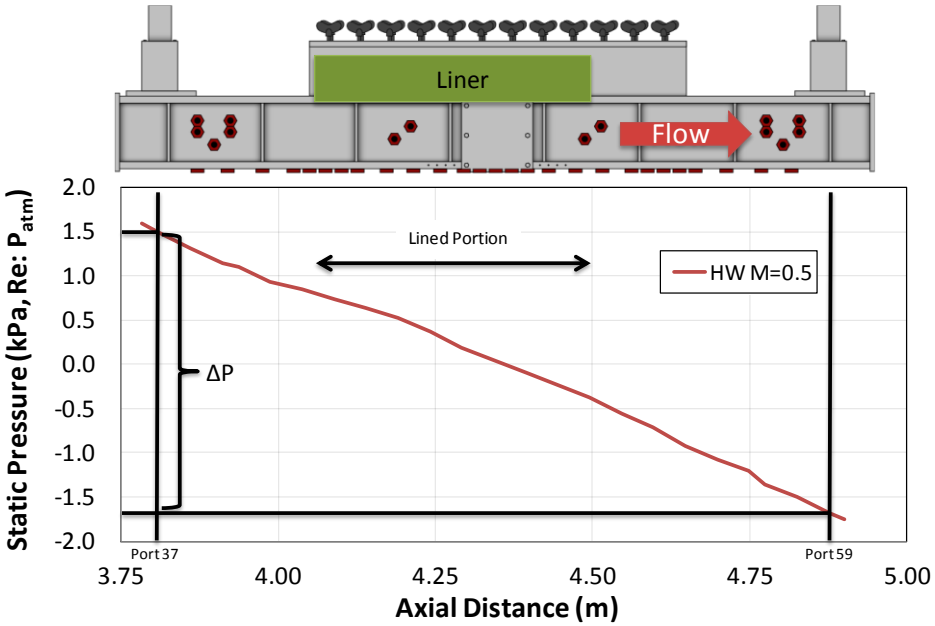

Figure 6. GFIT Test Section Static Pressure Distribution, Hardwall sample, M=0.5.

D.Measurement Process

Averaged static pressure measurements were made for each configuration with no acoustic excitation at M=0.1, 0.3 and 0.5. For each data set, 1000 readings from each static port were made over a nominal 40 sec period then averaged to give one measurement per port. Simultaneously, similar data were acquired from the high-accuracy gauge to provide the static pressure drop across the length of the liner. For all cases, the target Mach number was held to a tolerance of +/- 0.002 while static pressure in the test section was set within +/-130 Pa. Tunnel conditions, including average Mach number and static pressure, are also recorded to allow computation of λ from Eq. 2. Use of a non-dimensional coefficient like λ provides a benefit by normalizing the static pressure data. This normalization reduces the variability of the results, allowing comparison of data from different flow runs where static pressure and Mach number differences (albeit small) can affect the raw ΔP measurements. An example of this variation is shown in the left plot of Fig. 7 with a graph of ΔP measurements from the hardwall case at nominally M=0.5. The existence of a relationship between Mach number and ΔP is readily apparent. Computation of λ from this data results in the plots shown in the right plot of Fig. 7.

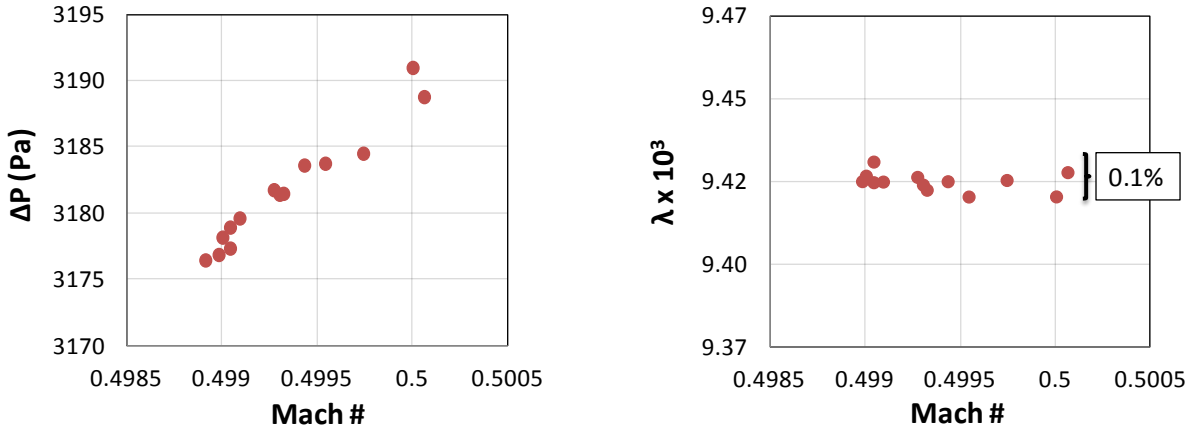

Figure 7. Liner ΔP measurements and corresponding values of λ, Hardwall sample, M=0.5.

The calculated values of λ are independent of the small Mach number changes observed while variability of the results about the mean is nominally 0.1%, indicating excellent repeatability. Comparisons with other flow speeds show variability decreasing with increasing Mach number, since ΔP increases while the accuracy of the pressure gauge is fixed as a percentage of its range. Note that values of λ derived from GFIT pressure measurements cannot be directly related to values of Darcy's friction factor commonly found on a Moody chart. Only a portion of the duct surface is lined and, depending upon M and the axial location of the test section, the flow may not be fully developed.

Tonal acoustic excitation was additionally used for M=0.1 to M=0.5 (0.2 increments) for frequencies between 400 and 2800 Hz (400 Hz increments) at a sound pressure level (SPL) of 140 dB (re 20μPa). In those cases, static pressure measurements were performed to evaluate the effect of acoustic excitation on liner drag. Acoustic measurements at M=0.0 were also performed to allow for comparison of liner impedances educed using the method of Watson[7] to the Two-Parameter prediction model provided by Jones.[8,9] Good comparison would improve confidence that the liner fabrication method (printed facesheets laid over a core) gives results similar to a conventional, fully-bonded, perforate-over-honeycomb construction.

IV. Results and Discussion

A. Static Pressure Measurements

Results of the static pressure measurements for each configuration are shown in Figure 8 for M=0.3 and M=0.5. The differences between the various configurations are small, varying by less than 50 Pa at M=0.3 to 120 Pa at M=0.5 (excluding the HW case). The static pressure drop does increase with increasing Mach number as expected and one can see the difference grow between the HW baseline and the liner configurations as M increases. The hardwall case produces the least pressure drop, as expected, while the remaining cases rank order by hole diameter with the smallest hole diameter producing the lowest pressure difference at both Mach numbers. Cavity depth effects on the measured pressure drop were minimal for all cases, implying that the facesheet geometry dominates the drag.

In Fig. 8, there are two plotted values for configurations using the S3 facesheet denoted by an asterix (*). During testing, it was observed that the downstream edge of the filler blank covering the last 152.4 mm of the core had bowed laterally downward into the flow causing a backward-facing step. This protrusion increased the measured pressure drop to a level comparable with the S2 configurations. The results were incongruent with expected trends and outside of measurement error band (+/- 0.7 Pa). The other configurations were tested significantly earlier (due to manufacturing complications with the S3 facesheet) and were not observed to have this bowing issue. A stiffer, metal filler blank was fabricated as a replacement and tested with the S3C1 configuration which reduced the measured pressure drop. Time restrictions prevented retesting for the S3C2 configuration.

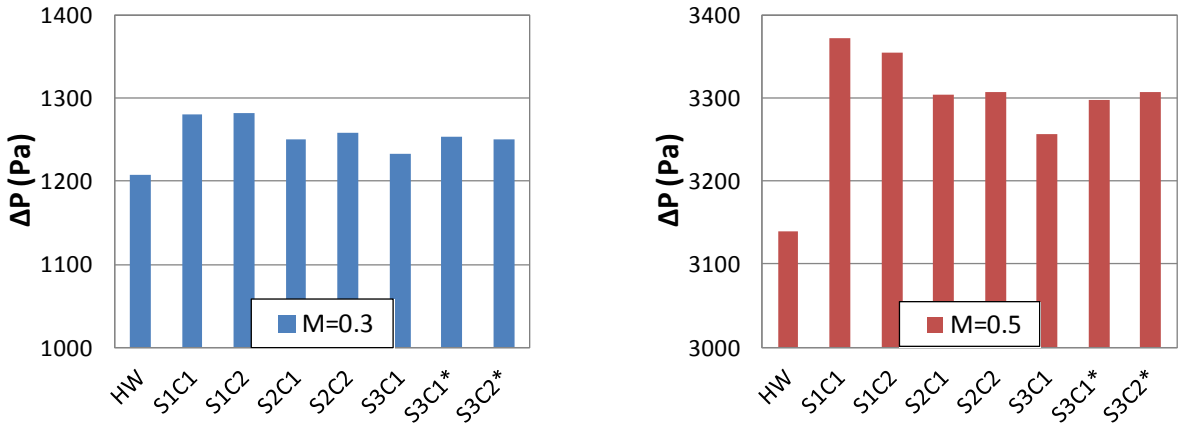

Figure 8. Measured static pressure drop (ΔP) for each liner configuration (no sound).

Using the pressure data and tunnel conditions to calculate λ results in Fig. 9 for the same Mach numbers and liner configurations. Values for the resistance factor decrease with increasing Mach number as shown by Nikuradse and the hardwall baseline produces the lowest values. As was observed for ΔP, λ decreases with decreasing hole diameter while changing cavity depth seems to have minimal effect on the computed resistance factor. The uncertainty of λ is of such small magnitude that error bars were not included in the figure. It should be noted that

variations between facesheets are significantly larger than measurement uncertainty while cavity depth effects are statistically insignificant.

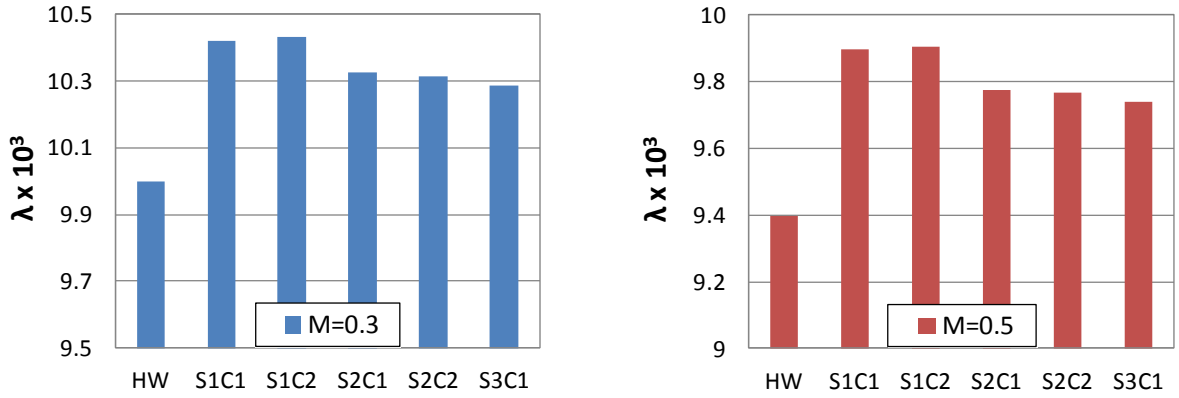

Figure 9. Resistance factor (λ) for each liner configuration (no sound).

B. Acoustic Measurements

Each liner configuration was tested in the presence of acoustic excitation at M=0.1, 0.3 and M=0.5 over the frequency range of 400 Hz to 2800 Hz with a SPL of 140 dB. Configurations with the C1 core also had full acoustic pressure profiles acquired at M=0 for the purposes of impedance eduction. These educed impedance spectra were compared to predictions made using the semi-empirical Two-Parameter model referenced earlier. Figure 10 shows results of this comparison for the S1C1 configuration. Good agreement is observed between the measured data and predictions. The largest divergence comes at the lowest frequency where liner attenuation is small making accurate eduction more difficult. The resistance spectrum is fairly flat across the entire frequency range while the reactance has the expected *-cot(kl)* shape.

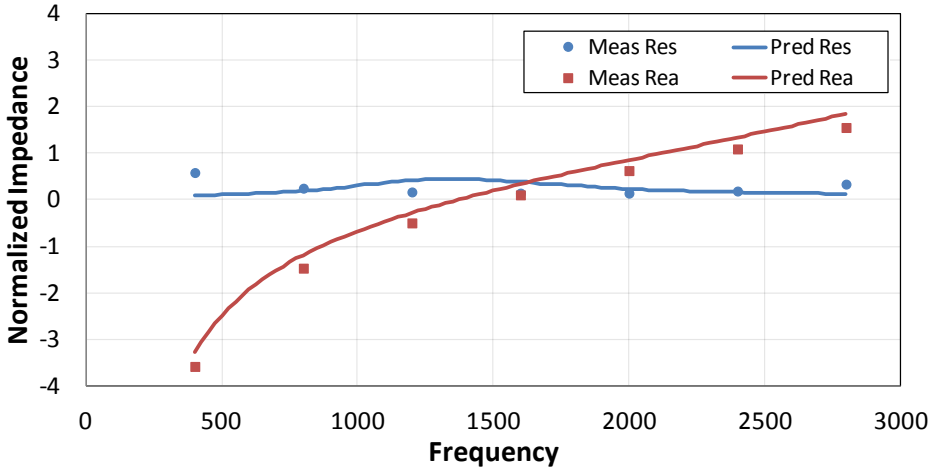

Figure 10. Comparison of Educed and Predicted Impedance, M=0.0, S1C1, 140 dB.

Figure 11 shows similar results for the S2C1 liner but with a greater discrepancy in resistance at the lowest frequency. Unlike the previous comparisons, results from S3C1 (Fig. 12) show a marked difference between the predicted and measured reactance. The measured values are lower than the predictions, particularly at the highest frequencies. This result would suggest the predicted anti-resonance frequency is lower than the measured one. Perforate hole size for this configuration (0.5 mm) was near the performance limit of the 3-D printer and although nominal hole size was verified using selected pin gage measurements, variability between holes over the length of the sample may be the cause of the difference. Overall, agreement between measurements and predictions was very good, especially for hole diameters greater than 0.5 mm. This gives confidence that 3-D printed liner facesheets, overlaid without bonding to the liner core, can produce acoustic results comparable to conventionally fabricated

liners. Such fabrication techniques will allow for rapid testing of facesheet geometries not easily duplicated by conventional machining.

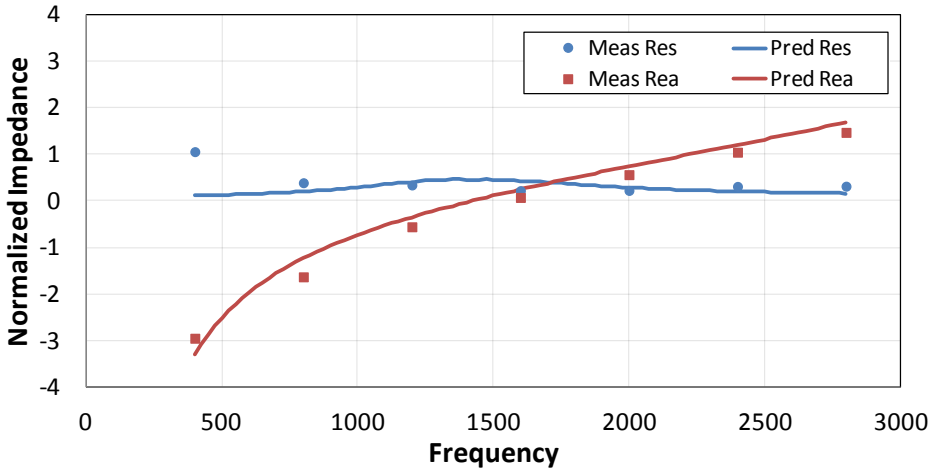

Figure 11. Comparison of Educed and Predicted Impedance, M=0.0, S2C1, 140 dB.

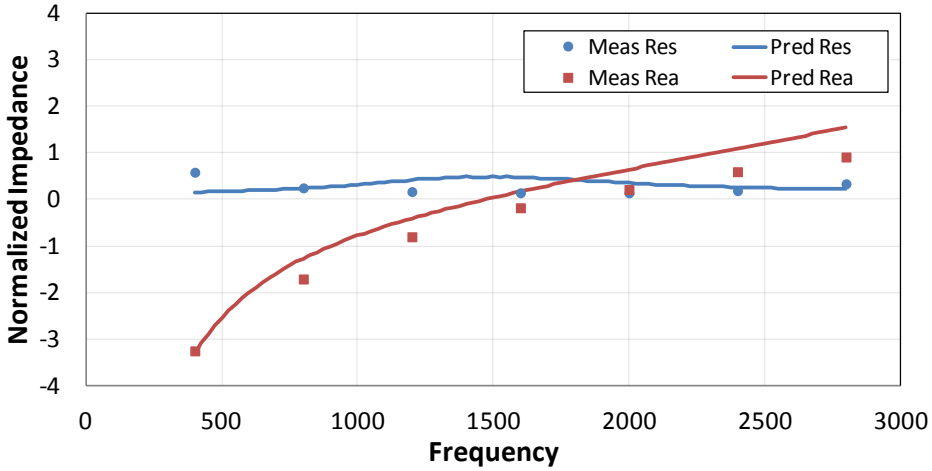

Figure 12. Comparison of Educed and Predicted Impedance, M=0.0, S3C1, 140 dB.

C. Effects of Acoustic Excitation on λ

Each liner configuration was evaluated in the presence of acoustic tonal excitation at an SPL of 140 dB from 400 Hz to 2800 Hz in 400 Hz increments to determine any effect on λ and, hence, drag. Results are shown at three Mach numbers: 0.1, 0.3 and 0.5 for each configuration. Figure 13 is a plot of resistance factor versus tone frequency for the S1 (largest hole) liners. For M=0.1, there is significant variability in λ with frequency at this sound pressure level but that effect seems to diminish entirely once the flow speed is raised to M=0.3. Data at M=0.5 shows similar insensitivity. Reducing hole size for the S2 liners does not seem to change the observed trends from the S1 configurations as shown in Fig. 14. Results from the S3 (smallest hole) configurations are given in Fig. 15 and are similar to the previous plots save for the S3C2 configuration at 1600 Hz. There, the computed value for λ is substantially higher than the rest of the M=0.5 values and even slightly higher than the M=0.3 values. Further scrutiny revealed that this data point was acquired during a series of repeat runs at selected frequencies necessary to fill in missing data due to an acquisition code malfunction. Thus, the data were acquired using the same bowed filler blank noted earlier. It was included to further show the effect of the bow and the importance of proper sample mounting while giving confidence that the rest of the dataset was unaffected.

The insensitivity to acoustic excitation observed at higher Mach numbers is a desirous result given the need for low cruise drag where flow Mach numbers in an engine inlet would likely be in a high subsonic range. At those Mach numbers, the required SPL to influence liner drag may be higher than levels typically found in a turbofan

engine. If inlet SPL's are sufficiently low, liner designs will not have to account for drag variation with frequency, thus reducing the number of optimization parameters required.

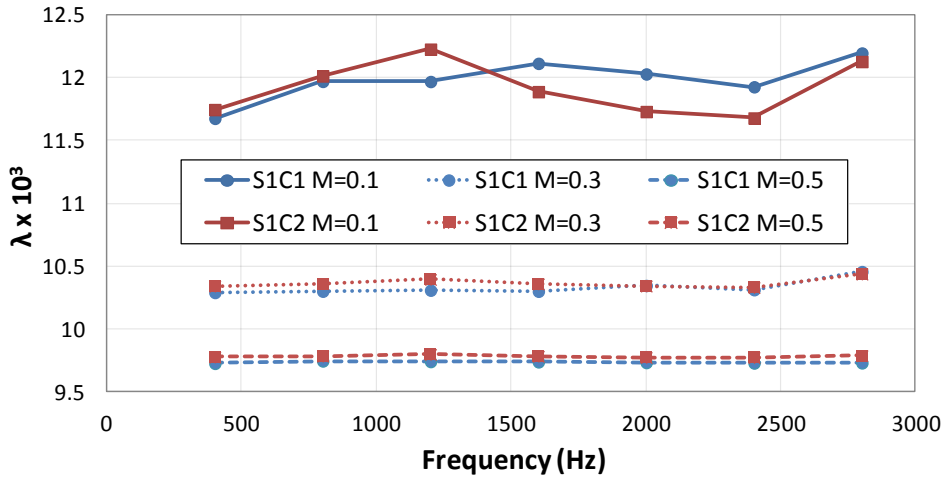

Figure 13. Resistance factor (λ) variation with source frequency and Mach number, S1 facesheet, 140 dB.

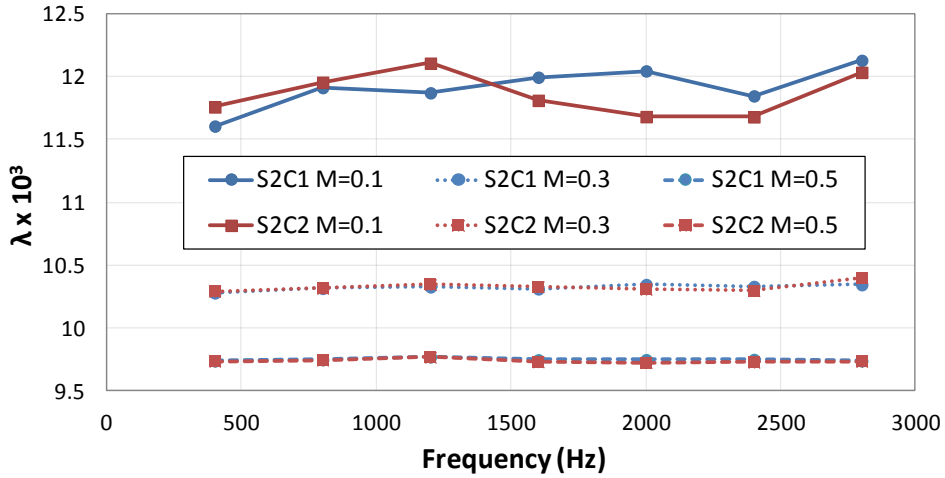

Figure 14. Resistance factor (λ) variation with source frequency and Mach number, S2 facesheet, 140 dB.

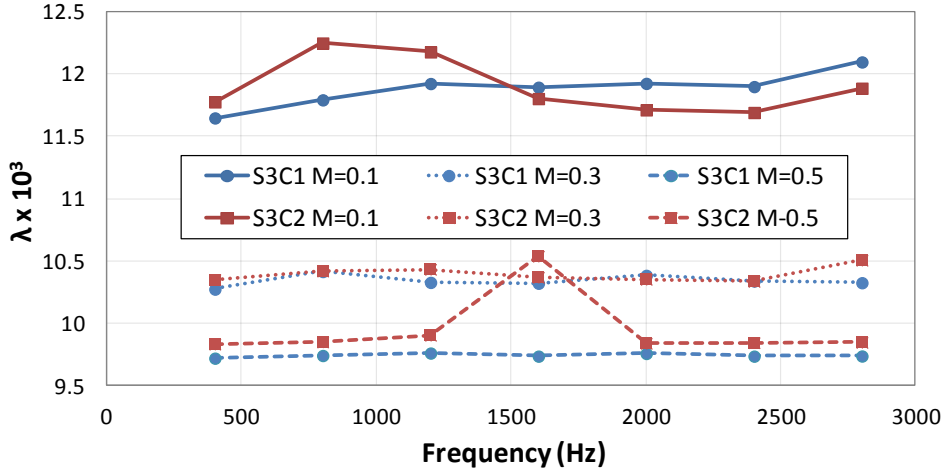

Figure 15. Resistance factor (λ) variation with source frequency and Mach number, S3 facesheet, 140 dB.

V. Concluding Remarks

An investigation was performed in the NASA Langley Grazing Flow Impedance Tube (GFIT) to evaluate the effects of perforate hole size and cavity depth on liner drag with and without acoustic excitation. Three facesheets were constructed of plastic resin using an stereolithography manufacturing process with three perforate hole diameters. These facesheets were overlaid on two conventional, metallic cores of differing depths to form six configurations. A hardwall sample was also included as a baseline case. Static pressure and acoustic pressure measurements were acquired for each configuration at Mach numbers up to M=0.5 with sound from 400 to 2800 Hz at 140 dB SPL. Educed impedances from the acoustic results at M=0.0 were compared to analytical predictions to evaluate the efficacy of the liner construction method. Analysis of the resulting data led to the following observations:

1. The static pressure drop, ΔP, measurement method detailed in this investigation can be used to determine the relative drag of various liner configurations in the GFIT. The simplicity of this method lends itself to rapid assessment of multiple liner configurations.

2. Use of the non-dimensional resistance factor, λ, in place of the measured ΔP, removes the effects of varying flow conditions that could result in day-to-day repeatability issues.

3. Increasing facesheet hole size increases the computed resistance factor values.

4. No significant effect on resistance factor was observed by varying the core depth for tests with no acoustic excitation. With excitation, there is a frequency-dependent variation in resistance factor, but the effect is reduced with increasing Mach number.

5. Predicted impedance spectra agreed closely with educed impedances from measured data, giving confidence that printed facesheets can be used to fabricate liners having acoustic characteristics similar to those of conventional construction.

Additional work is needed to relate relative differences in resistance factor to relative differences in liner drag. Ideally, values of the resistance factor could be correlated to absolute drag/unit area values. This result would require calibration liners tested in other facilities capable of performing direct measurements using a force balance.

Acknowledgments

The authors would like to thank Carol Harrison of the NASA Langley Structural Acoustics Branch for her efforts in collecting the experimental data along with Robert Andrews of the Advanced Fabrication Processes Section for his work in creating the liner facesheets. Funding for this effort was provided under NASA's Advanced Air Transport Technology Project for the Advanced Air Vehicles Program and by the Environmentally Responsible Aviation Project for the Integrated Aviation Systems Program.

References

[1]Tam, Christopher K. W., Pastouchenko, Nikolai N., Jones, Michael G., Watson, Willie R., "Experimental Validation of Numerical Simulations for an Acoustic Liner in Grazing Flow," AIAA Paper 2013-2222, 19th AIAA/CEAS Aeroacoustics Conference, May 2013.

[2]Drouin, M. K.,Gallman, J. M., and Olsen, R.F., "Sound Level Effect on Perforated Panel Boundary Layer Growth," AIAA Paper 2006-2411, May 2006.

[3]Thomas, R. H., Burley, C. L., Lopes, L. V., Bahr, C. J., Gern, F. H. and Van Zante, D. E., "System Noise Assessment and the Potential for a Low Noise Hybrid Wing Body Aircraft with Open Rotor Propulsion," AIAA Paper 2014-0258, January 2014.

[4]Wilkinson, S. P., "Influence of Wall Permeability on Turbulent Boundary-Layer Properties," AIAA-83-0294, AIAA 21st Aerospace Sciences Meeting, AIAA SciTech, 52nd Aerospace Sciences Meeting. January 1983.

[5]Roberts, D. W., "Equivalent Sand-Grain Roughness of Perforated Plate Acoustic Linings," AIAA-77-104, AIAA 15th Aerospace Sciences Meeting, January 1977.

[6]Nikuradse, J., "Laws of Flow in Rough Pipes," NACA TM-1292, November 1950.

[7]Watson, W. R., Jones, M. G., and Parrott, T. L., "Validation of an Impedance Eduction Method in Flow," AIAA Journal, Vol. 37, No. 7, July 1999, pp. 818–824.

[8]Parrott, T. L. and Jones. M. G., "Assessment of NASA's Aircraft Noise Prediction Capability, Chapter 6: Uncertainty in Acoustic Liner Impedance Measurement and Prediction," NASA TP 2012-215653, July 2012.

[9]Motsinger, R. E. and Kraft, R. E., "Design and Performance of Duct Acoustic Treatment: Aeroacoustics of Flight Vehicles; Chapter 14, Vol. 2: Noise Control," NASA RP 1258, August 1991.